QUANTIFICATION OF UNCERTAINTY DURING HISTORY MATCHING

A Thesis

by

MARTIN GUILLERMO ALVARADO

Submitted to the Office of Graduate Studies of
Texas A&M University
in partial fulfillment of the requirements for the degree of

MASTER OF SCIENCE

August 2003

Major Subject: Petroleum Engineering

QUANTIFICATION OF UNCERTAINTY DURING HISTORY MATCHING

A Thesis

by

MARTIN GUILLERMO ALVARADO

Submitted to Texas A&M University
in partial fulfillment of the requirements
for the degree of

MASTER OF SCIENCE

Approved as to the style and content by:

_____	_____
W. John Lee	Julian Gaspar
(Chair of Committee)	(Member)
_____	_____
Duane Mc Vay	Hans Juvkam Wold
(Member)	(Department Head)

August 2003

Major Subject: Petroleum Engineering

ABSTRACT

Quantification of Uncertainty During History Matching. (August 2003)

Martin Guillermo Alvarado, B.S., Universidad de Rosario

Chair of Advisory Committee: Dr. W. John Lee

This study proposes a new, easily applied method to quantify uncertainty in production production forecasts based on reservoir simulation. The new method uses only observed data and mismatches between simulated values and observed values as history matches of observations progress to a final "best" match. The method is applicable even when only limited information is available from a field. Previous methods suggested in the literature require more information than our new method.

Quantifying uncertainty in production forecasts (i.e., reserve estimates) is becoming increasingly important in the petroleum industry. Many current investment opportunities in reservoir development require large investments, many in harsh exploration environments, with intensive technology requirements and possibly marginal investment indicators.

Our method of quantifying uncertainty uses a set of history-match runs and includes a method to determine the probability density function (pdf) of future oil production (reserves) while the history match is evolving. We applied our method to the lower-Pleistocene 8-Sand reservoir in the Green Canyon 18 field, Gulf of Mexico.

This field was a challenge to model because of its complicated geometry and stratigraphy.

We objectively computed the mismatch between observed and simulated data using an objective function and developed quantitative matching criteria that we used during history matching.

We developed a method based on errors in the mismatches to assign likelihood to each run, and from these results, we determined the pdf of reservoir reserves and thus quantified the uncertainty in the forecast.

In our approach, we assigned no preconceived likelihoods to the distribution of variables. Only the production data and history matching errors were used to assess uncertainty. Thus, our simple method enabled us to estimate uncertainty during the history-matching process using only dynamic behavior of a reservoir.

DEDICATION

Dedicated to my wife, Carina, for her patience and to my two daughters, Maria Pilar and Amparo, aged eight and five, without whose loving attention this thesis would have been written in half the time; my mother, Raquel, for her continuous support; and finally my Uncle Jorge who inculcated in me a love for engineering.

ACKNOWLEDGMENTS

I would like to thank Dr. John Lee and Dr. Duane McVay, chair and member of my committee, respectively, for their continuous support and opinions. I also thank Dr. Thomas Blasingame for giving me the chance to join the Texas A&M Petroleum Engineering Department family; Dr. Hans Juvkam-Wold for his honest advice and support; my very close friends, Bjorn, Serguei, Christian, Marylin, Marcos and Georg, whose friendship made the two years at Texas A&M easier; and to the small Argentinean community of College Station whose endless barbecues and interested support have been fundamental for my family.

TABLE OF CONTENTS

LIST OF FIGURES

LIST OF TABLES

CHAPTER I

INTRODUCTION

In recent years the quantification of uncertainty has become critical in the petroleum industry because of the dominant role of capital intensive projects, complicated areas of exploration and possibly shrinking profits. The uncertainty in production forecasts (and associated reserve estimates) is directly related to decision and risk assessment in these difficult investment decisions.

Complete quantification of uncertainty in hydrocarbon production forecasts would involve full knowledge of all the variables involved in the determination of hydrocarbon volumes and flow and their individual probability distribution functions. Such detailed knowledge is rarely, if ever, available. Thus, the quantification problem is both important, and, as a practical matter, unsolved.

In the literature, several approaches have been proposed to deal with at least parts of the problem of quantifying uncertainty. Berteig, *et al.* [1] proposed a method to assess uncertainty of hydrocarbon pore volume associated with structure, porosity and permeability.

Others, including Floris *et al.* [2], Abrahamsen *et al.,* [3], and Samson [4] developed techniques to assess probability distribution functions due only to uncertainty in the position of the top structure. Floris *et al.* [5] focused their attention on quantification of the production forecast, just as we have in our study.

The main sources of uncertainties from a reservoir-engineering point of view are:

1. A model, which is commonly a poor mathematical representation of reality, uses a system of equations to try to simulate the dynamic behavior of fluid in an also imperfect static model.

_____

This thesis follows the style and format of *Society of Petroleum Engineers Reservoir Evaluation & Engineering*

2. Geological and fluid parameters are uncertain, because of a limited sampling of the entire space.

3. Errors are introduced by measurement procedures.

Given the broad spectrum of sources of uncertainty, a statistical treatment of the problem of assessing uncertainty given the lack of information about the reservoir and its properties is desirable. Despite this apparent need for statistical approaches, most production forecasts in practice are based on a single deterministic description of the reservoir that can reproduce with a certain quality and confidence the historic production and pressure data. The single deterministic model and its description make the model adopted and the associated production forecast rather subjective. The problem of determining the proper model, given outputs such as pressure and production data, is an inverse problem that has no unique solution.

Because uncertainty is inherently present in the production forecasting process, and because decisions must be made despite this uncertainty, there is considerable incentive to quantify this uncertainty. In this quantification effort, we must use the data that are actually available routinely. In our study, the data available were limited largely to an uncertain geological model and pressures and production data used for history matching.

Our proposed method is based on Bayesian inversion, but we had to modify the basic Bayesian approach to fill the gaps caused by limited available data. We illustrated application of our method with a set of 54 different history-match runs for an actual reservoir, with all history matches based on a single geological model.

These 54 runs reproduced the observed data with different qualities of fit. After each history match, we forecasted future production and we estimated the likelihood of each forecast using the deviation between simulated and observed data. We then used all production forecasts and their respective likelihoods to determine the pdf of expected reserves and estimated the limits of the 90% certainty range of production forecasts.

The reservoir that we used in this study was the 8-sand reservoir of the Green Canyon 18 field in the Gulf of Mexico. This reservoir is lower Pleistocene in origin and has complicated geometry and stratigraphy that includes a group of intercalated sands and

shales. The lateral extents of and connections between the flow units are unknown and thus represented an additional challenge during history matching. Given the geological complexity of the reservoir, not only were values of permeability and porosity uncertain; in addition, the positions of partial or total flow barriers and origin of the observed level of pressure support were unknown. Since the degree of uncertainty in the reservoir description was high, and the supporting data were scarce, no *a priori* probabilities of different descriptions could be considered in the quantification of uncertainty for this reservoir.

CHAPTER II

BACKGROUND

Reservoir management decisions have historically been based on predictions from a single-realization history-matched reservoir model. Uncertainty assessments are usually based on a sensitivity analysis on parameters considered most important in the model. However, to make a formal and complete estimation of uncertainty a full range of the distribution of the forecasted variable (such as reserves) is needed.

Many different variables of different kinds are involved in the total quantification of uncertainty in reserves estimation, including the variables that quantify geophysical, geological and fluid flow uncertainty. In this study, we focus on uncertainties arising in fluid flow modeling.

Floris presented a comparative study in which several research groups were asked to estimate the uncertainty in production forecasts from a synthetic case study. In this work, Floris described the different methods used by the different groups. Egbert *et al.* [6] presented a uncertainty quantification based on the maximum entropy method and using many different realizations of the reservoir that reproduced the historical data with satisfactory accuracy. Egbert *et al.* based their uncertainty quantification on 25 stochastic realizations obtained following more than 2,000 automated numerical simulations. Roggero[7] presented a new methodology that combines Bayesian formalism with the extreme scenarios. His methodology is used to identify the extreme behavior models for a given production forecasting behavior criterion (e.g., maximum and minimum reserves) that are equally probable. The difference between these two extreme production values is used as an estimation of uncertainty. Nepveu [8] presented an interesting approach based on Bayesian inversion with special application to cases where limited data is available.

These methods have many common features that we describe in this chapter.

Common Components

Fig. 2.1 is a general and useful flow chart that shows the common steps in the methods of quantifying uncertainty published by the authors summarized above.

	ESTABLISH INITAL MODELS
	SELECT PARAMETERS
POR, PERM	DETERMINE A PRIORI DISTRIBUTIONS OF PARAMETERS
SIMULATOR	SIMULATE FIELD PERFORMANCE
	COMPARE SIMULATE AND OBSERVED DATA
OPTIMIZER	CALCULATE OBJECTIVE FUNCTION AND OPTIMIZE RESULTS
	OBTAIN BEST MATCH
	ESTIMATE UNCERTAINTY
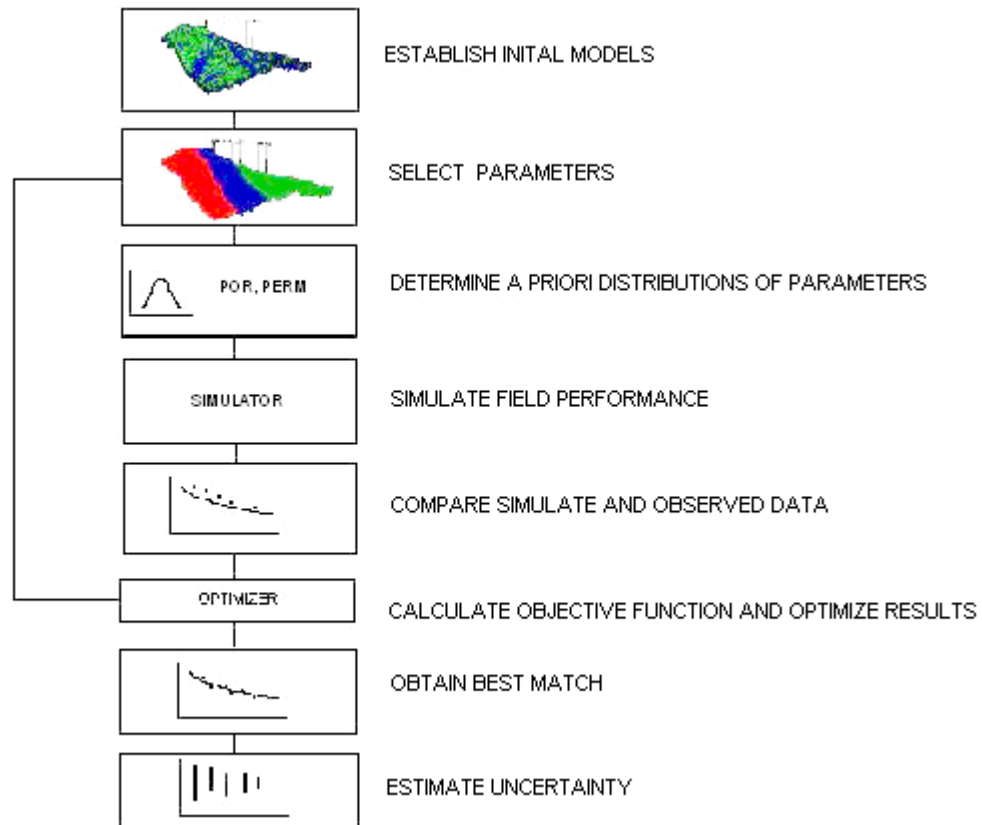
Fig. 2.1—Flow chart used by most existing methods to assess uncertainty.

Six components are common to all the methods we cited that assess uncertainty using production data.

- Probability distributions of parameters and their geographic characteristics (i.e., global, regional, pilot point).

- Parameterization.

- Objective function, which quantifies the mismatch between simulated and observed data.

- Posterior distribution determination.

- Optimization algorithms that may vary from manual history matching to complicated optimization algorithms.

- Uncertainty determination algorithms.

A priori **model.** The initial, or *a priori*, model is based on previous experience, measurements and geological knowledge. Uniform distributions of variables can be assumed when only limited data are available.

Parameterization. Parameterization is the method we use to modify our reservoir model to condition it to the available production data. Parameterization usually means adjustment of the spatial distribution of permeabilities and porosities within the model to obtain a better match of observed data.

There are different approaches to parameterize the spatial distribution of variables. Some of them are more suitable for later use in the optimization phase.

Individual Grid Blocks. The most general and probably the oldest method is to consider the values of the adjustable parameters in all the grid blocks to be independent parameters. The limitations of this approach are that we may not using our previous knowledge of deposition and we may not honor known discontinuities in the reservoir and the need of a massive computer resources. Furthermore, this method is not suitable for use with automatic optimizers.

Regions. The use of different regions in a reservoir is a common method to reduce the number of variables involved in the matching process. Use of regions allows us to incorporate, in some degree, geological knowledge of the reservoir. Appropriate regions can be defined to account for layers, impermeable barriers and drainage areas of wells. Generally, the reduced number of regions may not be sufficient to describe the actual heterogeneities and may generate some abrupt changes at borders of the regions.

Pilot Points. As discussed by Ramarao [9], hydrogeologists developed the pilot point method to assess uncertainty in their predictions of groundwater flow and contaminant transport. The innovative aspect of the Pilot Point method is the generation of a number of conditional simulations of the transmissibility preserving statistical moments and the spatial correlation structure of the measured transmissibility field while honoring measured transmissivities at their locations.

The original pilot point method consists of three main stages. First, using all observed information, we determine the parameters of the statistical characterization of

the transmissibility (mean, variance and covariance). In the second stage, we estimate the transmissibility field by co-kriging. In the third stage, we generate conditional simulations of the transmissibility field.

Briefly, the pilot point technique provides an objective method to solve inverse problems. It consists of calibrating an initial co-kriged transmissibility field, generated from the observed values of transmissivities, and generating a set of synthetic transmissibility data at selected unmeasured locations referred to as pilot points. Ramarao proposed a method to select pilot points. The pilot points are generally at locations with large uncertainties in reservoir properties.

This pilot point method solves most of the problems presented by the regions approach.

Global Parameters. Other methods that cannot be linked to specific locations are called global parameter methods. An example of these methods is the gradual deformation method described by Manceau.[10]

Objective Function. We use the objective function to determine the extent to which the behavior of our model differs from the observed data. In automatic history matching, the objective function is recalculated in each loop in which values of porosity and permeability are varied. The definition of objective function will depend on the observed variables available, the purpose of the study, and on the way chosen to normalize the function. The objective function usually provides a way to assign more relative weight to certain observed data than to others.

In the literature, we commonly find studies performed using objectives functions based on squared values of the difference between simulated and observed values and normalized using the standard deviation of measurement errors. For example, Egberts *et al.* used the root mean square as an objective function while Roggero [11] used a sum of the different variable terms an a matrix of covariance to account for the errors in simulation and in measurement.

The most common function to describe a mismatch can be stated as:

$$\sum_{observed\ \mathbf{data}} \left\{ Weight \times \left(\frac{Observed - Simulated}{StdDev} \right) \right\}^2 \qquad \ldots\ldots\ldots\ldots\ldots\ldots(1)$$

StdDev represents the standard deviation of the measurement errors. *Weight* is the relative weight assigned to each different kind of production parameter.

Optimization algorithms. Optimization algorithms are intended to produce models that closely reproduce the observed production data. Manual history matching is performed by trial and error using reservoir knowledge, judgment and the visual quality of the match. In contrast, most approaches currently used in inversion problems involve an automatic generation of values and a recalculation of objective functions through the use of an optimization algorithm.

The most-used algorithm is the gradient method. This approach can be used with smooth functions and when the objective function can be assumed to vary linearly with parameter changes. Disadvantages of this method include the possibility of converging to a local minimum in the objective function and the long computing time required to perform the gradient calculations. Still, the gradient method can be used to improve the efficiency of the inversion process. For example in the pilot point method, the gradients of the simulation results at the pilot point values are used in the optimization algorithm.

Others methods like genetic algorithm and simulating annealing can be used for optimization. Simulated annealing minimizes the deviation between the grid statistics and target values; this deviation function is usually called the "energy" of the objective function. Simulated annealing uses a special algorithm to minimize the energy function, implying that the difference between the target and grid statistics has been minimized. As a simple example, the objective can be to synthetically produce a sand/shale model with a net-to-gross ratio of 70%, an average shale length of 180 ft and an average shale thickness of 30 ft. The model starts randomly distributing sands and shales with the specified ratio of 70% and then swapping and iterating trying to reach the target conditions. This method has also been applied to fit geostatistical models to production data.

Uncertainty Quantification. Uncertainty quantification can be classified in two main categories: maximum likelihood models and methods using multiple models. Maximum likelihood models include single value forecasts, which do not provide uncertainty quantification, and the gradients method. These methods are based on the computation of gradients in selected production variables described with parameter data types. If we know the error distribution of the reservoir parameters we can estimate the uncertainty of production variables. Limitations of this method are that (1) the **relationship between predicted quantities and the reservoir model parameters must be linear; (2) the error distribution must be known; and (3) the model error must be negligible.**

Methods using multiple models include Monte Carlo simulation, the extreme scenarios method, and Bayesian inversion. Monte Carlo simulation allows the inference of a probability distribution of a function from a massive random generation of values of the input values.

The extreme scenarios method consists of finding extreme, equally probable forecasts forecasts corresponding to a most optimistic and a most pessimistic scenario. The uncertaintly range is simply the difference between those two extremes. Roggero[7] notes that the algorithm that implements this method can be formalized to be the search for models that identify both (1) Min (Matching Criterion) + Max (Forecasting Criterion) and (2) Min (Matching Criterion) + Min(Forecasting Criterion).

Other methods using experimental design theory and Response Surface Methodology (RSM) can also be used to reduce dramatically the number of simulations and make the optimization process simpler.

The purpose is to approximate a complex process with a regression polynomial that approximate the process within a certain region. The advantage of the method is its negligible cost to estimate new values of responses compared to time consuming reservoir simulations.

The disadvantage of this approach is the implicit assumption of the validity of the response surface methodology in that space.

The Bayesian inversion approach systematically combines prior knowledge and experience with a system to improve a prediction. In this way Bayesian inversion does not rely solely on the size of the data sample. Bayesian inversion is one of the most widely used techniques in inversion problems.[12] It is based on theorem from probability theory first proposed by the eighteenth-century English country clergyman and philosopher Thomas Bayes. To understand this theorem, let B_1, B_2, …, B_n, be n mutually exclusive and collectively exhaustive outcomes of some event B. Let A be an outcome of an "information event" or a "symptom" related to B. Note that A is not perfect information; it simply correlated to the event B. When A is perfect information about B, Bayes' theorem is not needed, but, in the more usual case, A is just a symptom that contains information useful in revising our prior probabilities about B. The revised probabilities are calculated using **Eq. 2**.

$$P(Bi/A) = \frac{P(A/B_i)P(B_i)}{\sum_{j=1}^{k} P(A/B_j)P(B_j)} i = 1,2,....k \; \dots\dots\dots\dots\dots\dots\dots\dots\dots\dots\dots\dots(2)$$

$P(A/B_i)$ is the conditional probability of event A occurs when B_i event has happened.

$P(B_i)$ and $P(B_j)$ are respectively the probability of events B_i and B_j

The result $P(B_i/A)$ is also called the *probability of the causes*. Bayes' theorem can be used in many applications in which we need to access the probabilities of the causes. For example, Bayesian inversion has achieved strong popularity in geophysical inversion problems.

Scales [13] explained the use of Bayes' theorem philosophy as follows. Suppose by previous work we know something about a model (e.g., from previous experience) before using available data. The prior knowledge and conjectures are called the *a priori* model. This knowledge is transformed into likelihoods or probabilities. Often likelihoods are assumed to follow a Gaussian distribution. Suppose we then have a set of data and also the statistical parameters describing the data (variance and covariance). The Bayesian approach provides a method to fine-tune the *a priori* model with the set of

available data. The posterior distribution tells us how the data correct the prior knowledge.

Nepveu [8] provides the key point of assessing uncertainty when only limited data are available. He presents the problem starting with the conditional probability derived from Bayes' theorem.

$$P \text{ (parameters}/p) = P \text{ (}p/\text{parameters) x } P \text{ (parameters) } / P \text{ (p)} \dots\dots\dots\dots\dots(3)$$

P (parameters) is the *a priori* distribution, P (p/parameters) is the likelihood of the model with parameters values *parameters*, P (parameters/p) is the conditional probability that the chosen parameters pertain to the real reservoir given the error p calculated with the objective function, and P (p) is the probability that error have a value p, and serves as a normalization factor.

When only limited data about the reservoir are available, we can assume a constant probability distribution and **Eq. 3** becomes:

$$P \text{ (parameters}/p) \text{ is proportional to } P \text{ (}p/\text{parameters)} \dots\dots\dots\dots\dots\dots..(4)$$

In the PUNQ (**P**roduction Forecasting with **Un**certainty **Q**uantification) studies, the authors assumed this likelihood to be Gaussian. It is then expressed as:

$$P \text{ (parameters}/p) = \exp(-p) \dots\dots\dots\dots\dots\dots\dots\dots\dots\dots..(5)$$

Theoretically, the error may assume values from zero to infinity, and the probability function can be expressed as

$$pdf\left(\mu\right) = \int_{0}^{\infty} P\left(\frac{\mu}{p}\right)\exp(-p)dp \dots\dots\dots\dots\dots\dots\dots\dots\dots\dots\dots\dots(6)$$

$P(\frac{\mu}{p})$ is the conditional probability that the reservoir will produce an ultimate volume μ given a error p.

Eq. 6 does not appear to be helpful unless there is sufficient information to determine P(μ/p). If we knew all the produced hydrocarbon volumes μ for all values of p, we could determine the pdf(μ) by using **Eq. 6**. The problem is that we do not have values of

hydrocarbon production for all the error values. Fortunately, there are two ways to compute the probability density p(μ/p) using the maximum entropy method:

First, if there are a large number of a reservoir models, we can subdivide the error interval into bins and calculate the average production average and standard deviation for each bin. In this case, the maximum entropy solution for P (μ/p) in that bin is the Gaussian Distribution N(μ,σ)

$$P\ (\mu/p) = N(\mu,\sigma) \dots\dots\dots\dots\dots\dots\dots\dots\dots\dots\dots\dots\dots\dots\dots\dots\dots\dots(7)$$

Second, when only sparse data are available, we select a value of production from the reservoir and assume or estimate the minimum production associated with that error. Once we set a scale parameter $\lambda(p) = m - m_{min}(p)$ then the maximum entropy distribution will be given by:

$$P\ (\mu/p) = (1/\lambda(p))\exp(-\mu/\lambda(p))\ \text{for}\ m >= m_{min}\ (p)\ \dots\dots\dots\dots\dots\dots\dots\dots(8)$$

For values of p for which no model is available we must interpolate. The limitation of this method is that the uncertainty calculation can be no better than our estimate of minimum production.

CHAPTER III

METHODOLOGY

I evaluated my proposed method to assess uncertainty using a sequence of manual history matches of the 8-sand reservoir in the Green Canyon Block 18 field (GC-18). The objective was to quantify the uncertainty of cumulative oil production forecasts during the history matching process and to obtain a realistic estimate of the uncertainty once the matching was considered finished.

The GC-18 field, located some 90 miles off of the Louisiana coast, was discovered in early 1982 with well GC-1. All the wells in Green Canyon were drilled from a single platform with a water depth of 760 feet.[14]

The GC-18 field came on stream in May 1987. To date, 30 wells have been drilled, of which 26 penetrated the 8-reservoir while only 8 penetrated the reservoir's hydrocarbon bearing areas. Despite being penetrated by so many wells, the extent of the 8-reservoir is still unknown and the positions of its fluid contacts, if they exist, have never been determined. Production from the 8-reservoir has been from six wells: wells 2, 3, 6, 7, 12, and 25.[14]

The reservoir is composed mainly of sand/shale intercalations that degenerate to inches-thick laminations at shallower depths. Geologists agree that the reservoir was geopressured by post-accumulation tectonic events. However, the amount of pressure support in the reservoir is not consistent with the original overpressure. Geologists explain the higher-than-expected pressures in different ways, including communication with other reservoirs, responses of confined shales, or under-estimation of reservoir size.

An M.S. student in petroleum engineering at Texas A&M University modeled the reservoir with a commercial reservoir simulator using 45,000 grid blocks.

Fig. 3.1 shows a 3-D view of the porosity distribution. Areal distribution of porosity and position of the fault are shown in Fig. 3.2.

Figs. 3.3 and 3.4 show the horizontal permeability distribution in areal and cross section maps respectively.
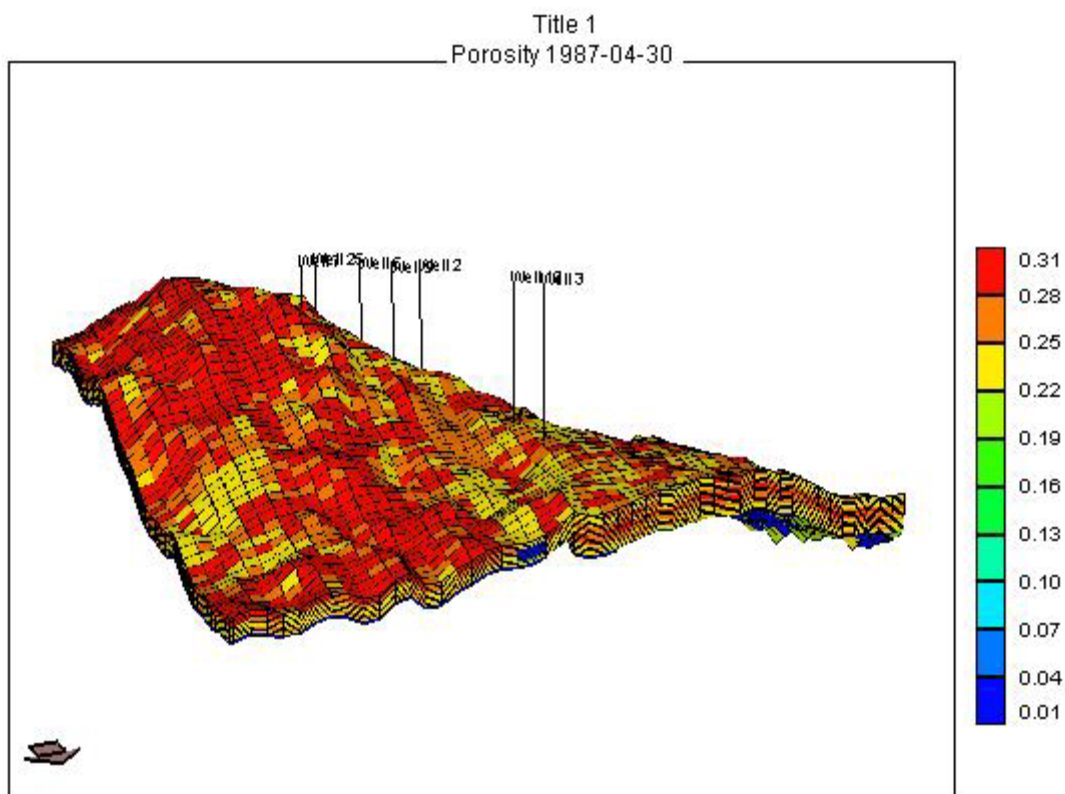
Fig. 3.1— 3D image of the Green Canyon 18 8-sand reservoir model.
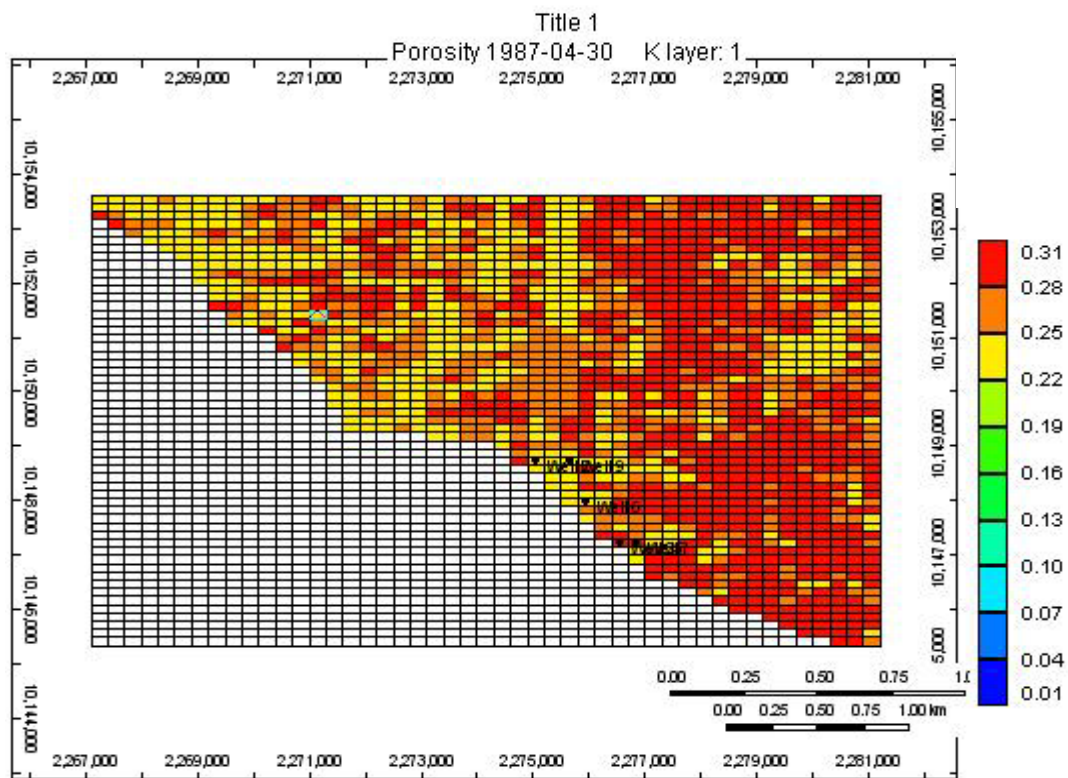
Fig. 3.2—Areal view of the model and its porosity distribution.
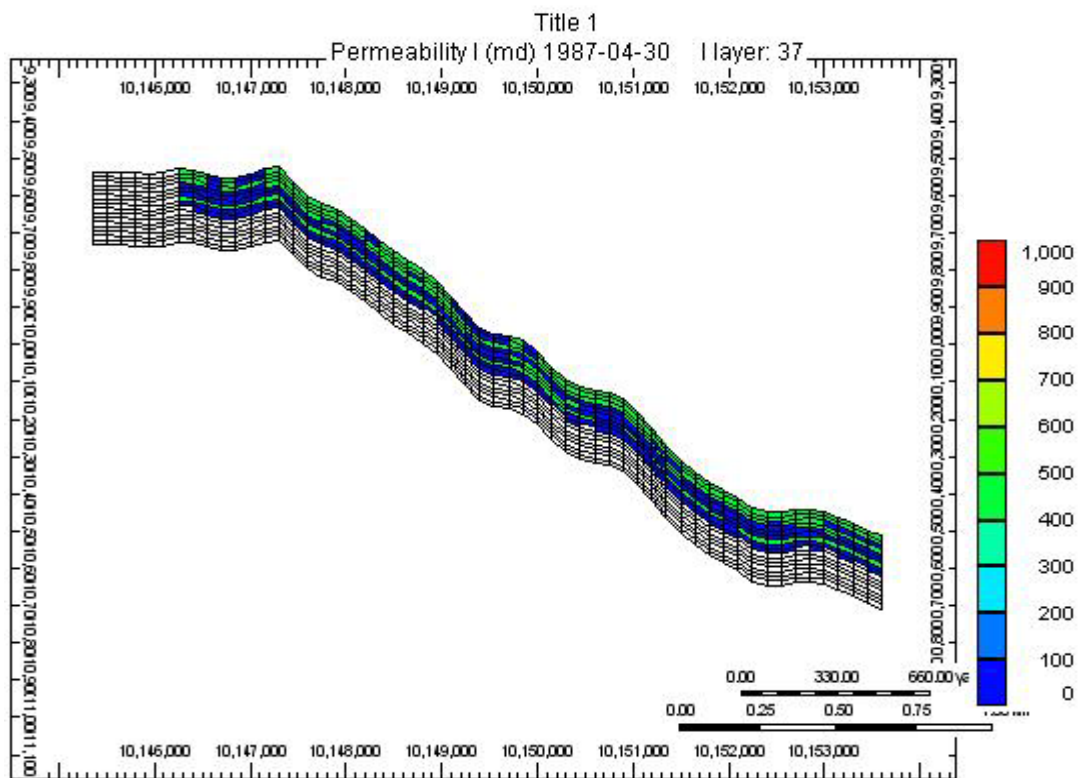
Fig. 3.3—Cross section of Green Canyon 18 8-sand reservoir model and its permeability distribution.
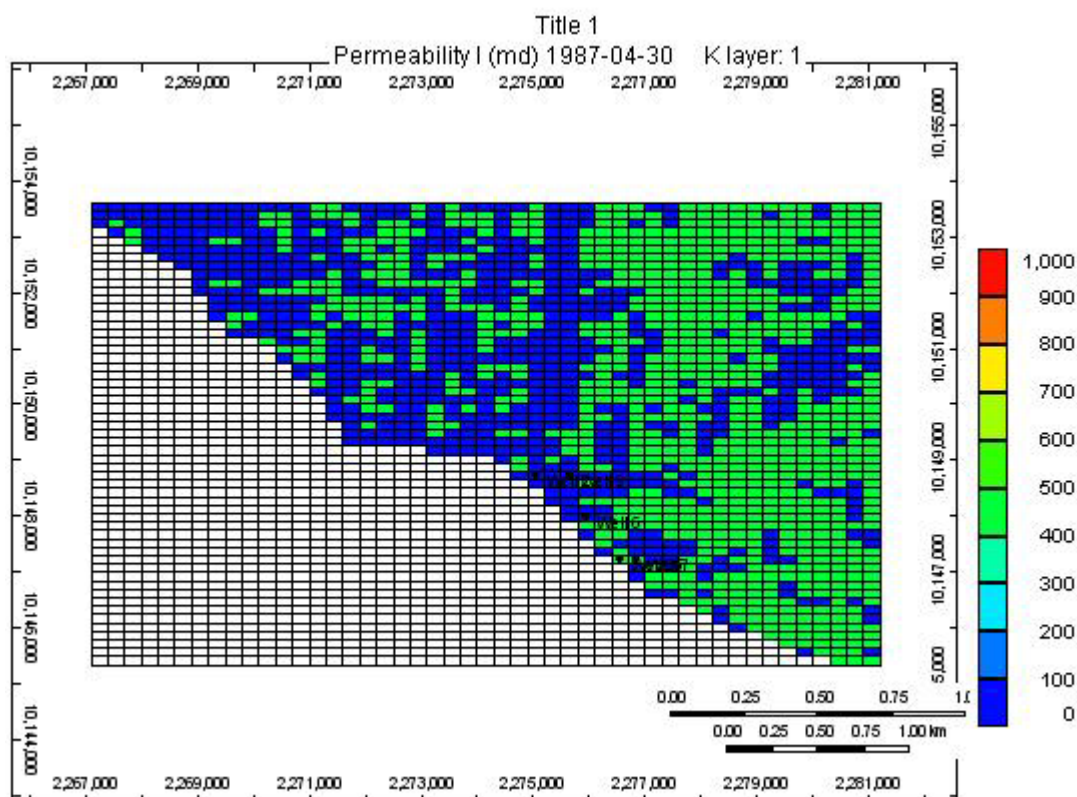
Fig. 3.4—Areal view of the model and its permeability distribution.

Observed data available for history matching consisted of static pressures from wells 3, 6, 7 and 12, and field oil, water, and gas rates from 1987 to 2001. Some wells were shut in suddenly and unexpectedly during the production history of the field because of sudden increases in sand compaction. The results of those unexpected failures can be seen clearly in **Fig. 3.5.**
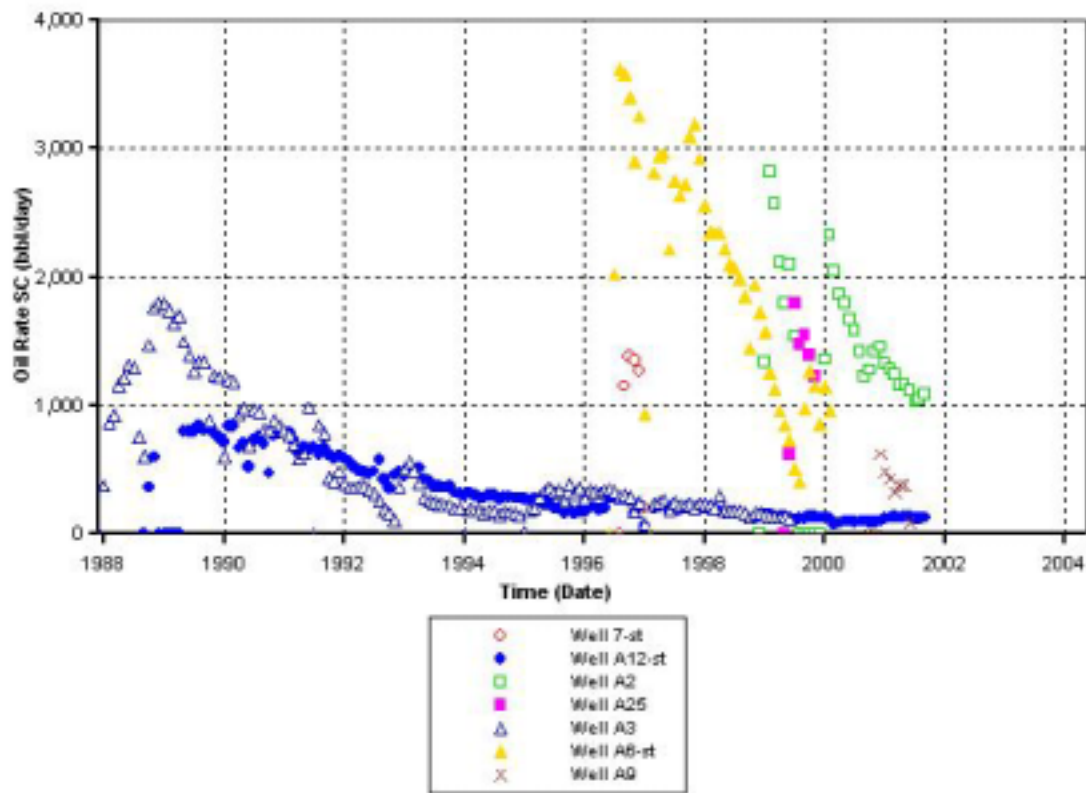
Fig. 3.5—Oil rates with unexpected shut-ins due to casing failures.

The history match consisted of 53 different runs, each followed by a visual comparison comparision of observed and simulated pressures, water cuts, and gas/oil ratios. During the many runs different zones were established to modify the simulated reservoir performance and to attempt to match observations better. **Table 3.1** presents a description of and some comments about some history-match runs.

TABLE 3.1 – MODIFICATIONS DURING HISTORY MATCHING

RUN	Comments
3	No water simulated water production -

TABLE 3.1 Continued

RUN	Comments
4	Well 2 located in permeable layer
6	Net to gross ratio reduced, oil compressibility reduced
8, 9	Fluid barriers reducing vertical permeability
10	Added pinchouts at the west and east
11,12,13,14	Re-perforation intervals at wells 2, 6 and 12, trying to get better water matches
15	Increased permeability – better water match
16	Same as 14 with barrier to the east and west.
18	Increased net to gross from run 16
19	Introduced permeable barrier beyond Well 12 from run 14
20	Reduced perforated interval in well 12
21	Reperforation schedule in wells 3,5,7 and 12
22	Using run 14 new reperforation schedule in wells 3,5,7 and 12
23	Increased net to gGross from run 21
24	Well 3 is perforated in layer 12
25	Vertical permeability increased to 0.1 mD
26	Modifications in perforations of wells 3 and 2
27	Removed flow barrier (Sector2), well 3 perforated from bottom layers
28,29	Reperforations in wells 3 and 12
31	Removed perm barrier in layer 7 from run 26.
32,33,34,35	Perforated intervals of wells 3 and 12 have been reduced at early times
36,37	Removed barrier in layers 1 and 2.
39	A barrier in layer 7 has been set from run 36
40,41	Reduced vertical permeability
42	A barrier in layer 7 was re-introduced from run 37

TABLE 3.1 Continued

RUN	Comments
44,45	A barrier is introduced in layer 2 from run 37
46	Increased vertical permeability in western area
49	Increased thickness of layer 4
53	Vertical permeability in layer 9 = 0 from run 49
54,55,56,57	Vertical permeability in layer 9 = 0 from run 36

We defined an objective function to describe the quality of the observed mismatch in the history-match runs. The literature includes a number of definitions of objective functions, usually with broad similarities.[2] Because we were working with a completed history-matching project, we designed our objective function to simulate or capture the visually observed mismatches and also to help us determine which parameters were given more emphasis in the manual history matches. **Fig. 3.6** to **Fig. 3.8** illustrate some representative history-match runs (numbers 3, 16, 30, and 39) in which the improvements in the matches (especially pressure) can be readily observed.

Ultimately, we used most of the available information to determine the mismatch between the simulated and the observed data. We included in the objective function: water cuts (WCT) of wells 2, 3, 6, 7, 9,12, and 25; gas/oil ratios (GOR) for the entire field; and static pressures (BHP) of wells 3, 6, 7 and 12.
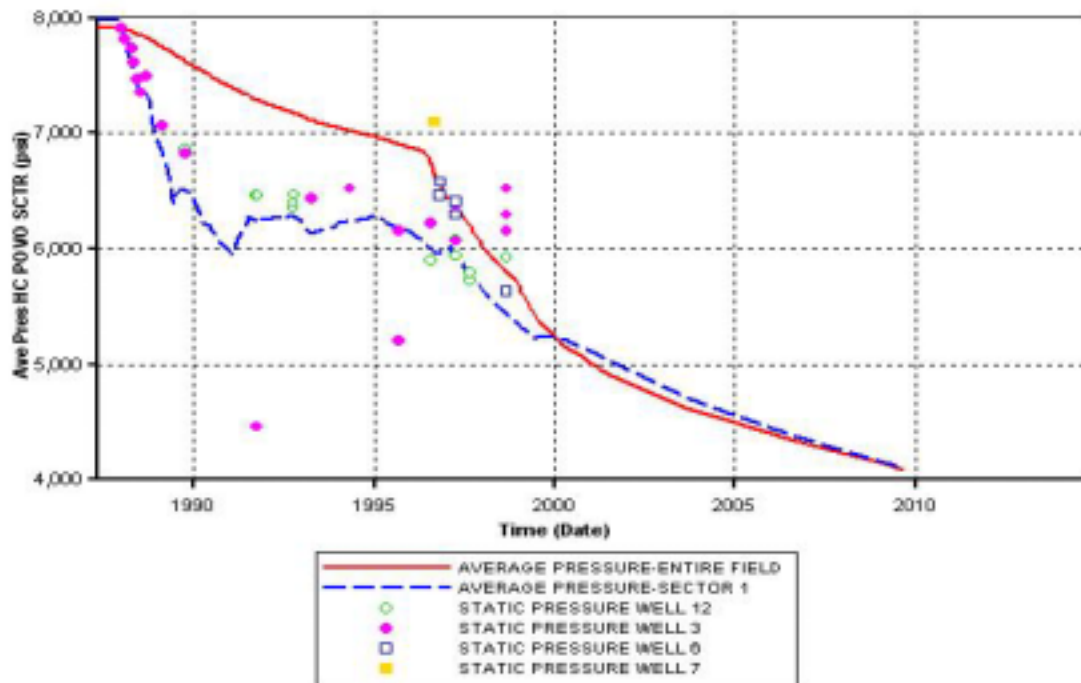
Fig. 3.6—Simulated average pressures and observed static pressures.
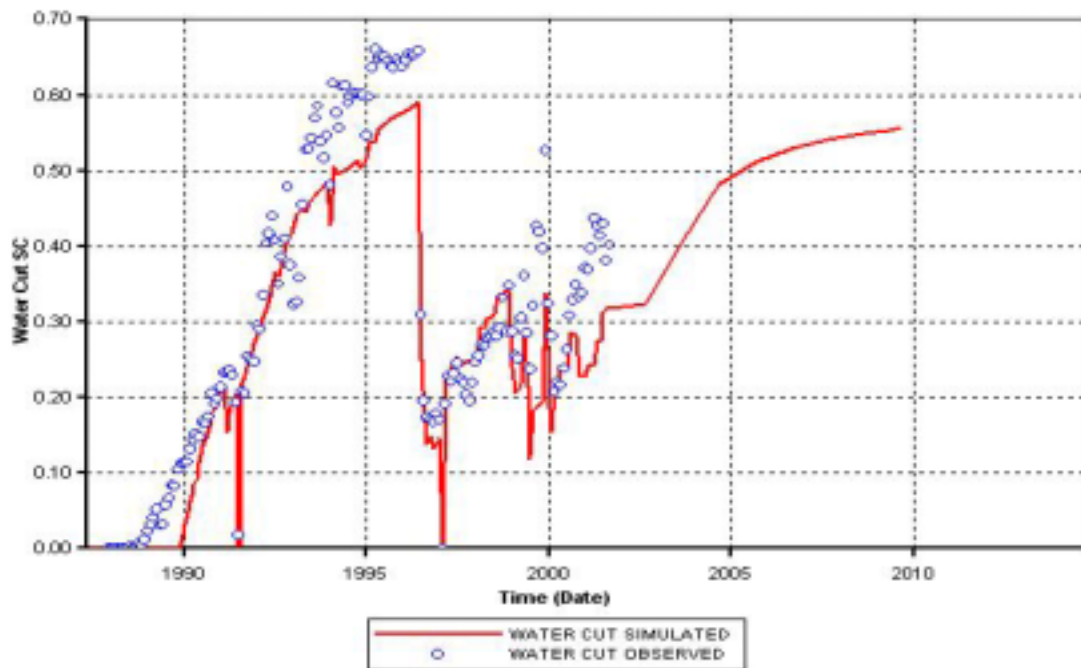
Fig. 3.7—Simulated and observed water cuts.
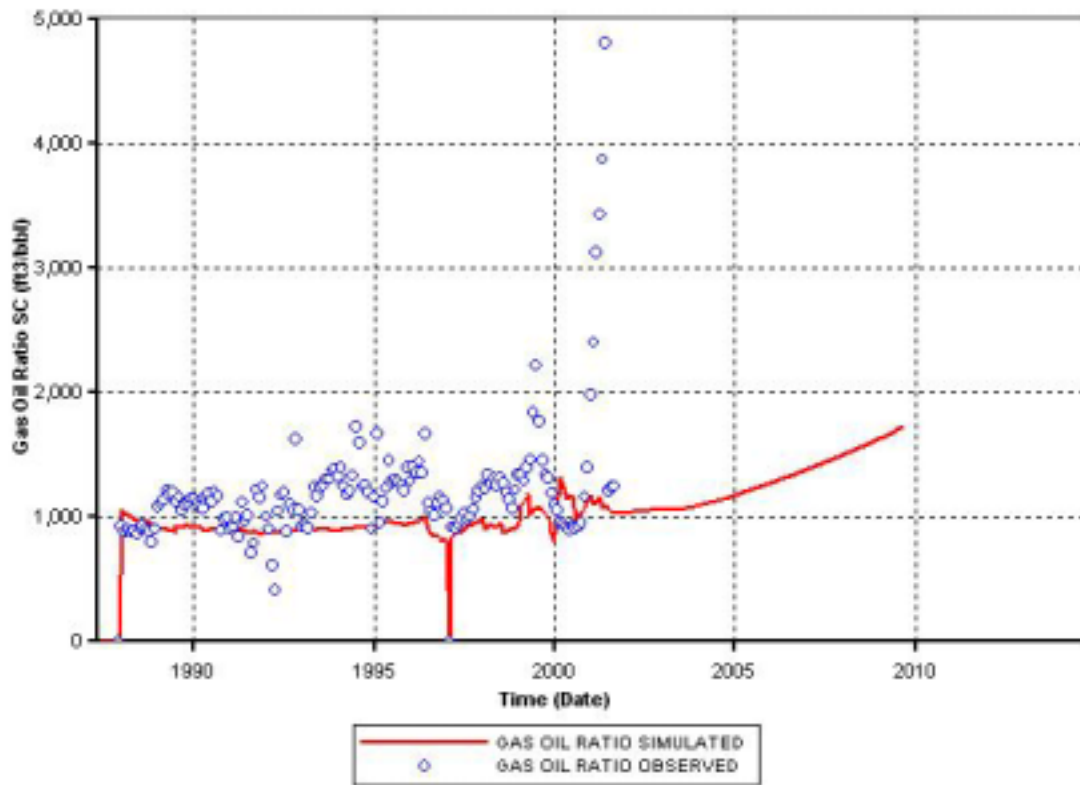
Fig. 3.8—Simulated and observed GOR, showing no important improvements during history matching.

In each time step in which observed data were available, we computed the absolute value of the difference between simulated and observed data. We then summed these differences and normalized them with the observed values so that we could sum errors from different sources. Since the number of observations was not the same for all variables we had to divide the sum by the number of observations to avoid dominating some infrequently observed variables with the more frequently observed ones. We divided by the sum by the number of actives wells. Our normalized error calculation then took the form

$$Error = \frac{1}{n_w} \sum_i w_p \frac{1}{n_p} \sum_j \frac{1}{n_t} \sum_k \left| \frac{v_{sim} - v_{obs}}{v_{obs}} \right| \quad \dots\dots\dots\dots\dots\dots\dots\dots\dots\dots\dots\dots\dots\dots\dots\dots\dots\dots(9)$$

v_{sim} and v_{obs} represent simulated and observed values of a variable at the same time step.

In **Eq. 9**, subscripts i and j run over the wells and production data types while k runs over the different time steps. The weighting factor w_p represents the weight given to a variable relative to the others. We gave 70% weight to the error in BHP error, and 15% each to WCT and GOR. We selected these weighting factors to quantify the intuitive weights given by the student who performed the history matching. Egberts *et al.* [6] reported a similar approach.

Runs 21, 26, 28, 29, 32, 33, 34 and 35 were further efforts to match early data. To take into account the special importance of matching early data, we introduced a weighting factor, e_k. We tried values of 1, 1.5 and 1.7 for early times for this factor and required that the factors for later data sum to unity to avoid modifying the balance between the
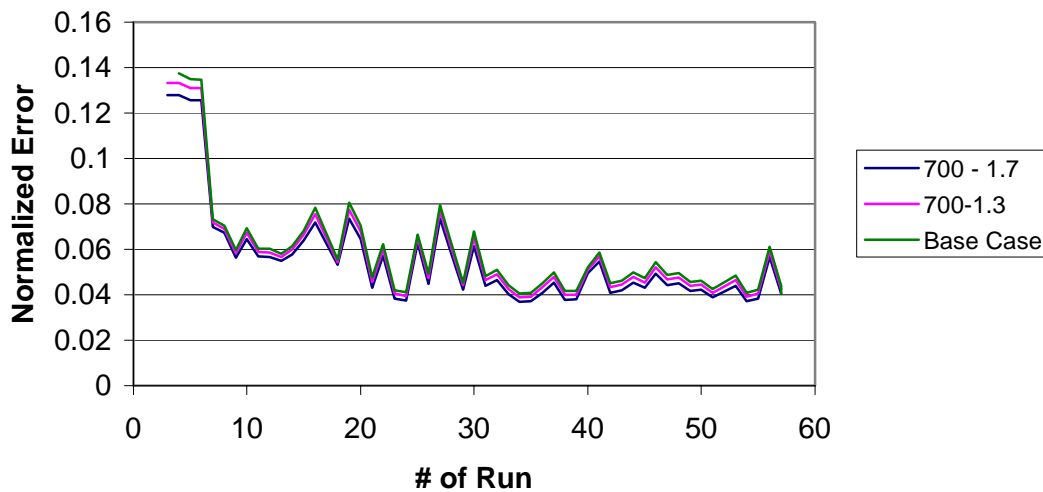
Fig. 3.9—Emphasizing earlier data reduced total error.

different variables. **Fig. 3.9** shows the sensitivity of the calculated errors to different factors for weighting the early data.

We also need a definition for "early time." We used and analyzed three different values: 700, 1,500, and 3,000 days.
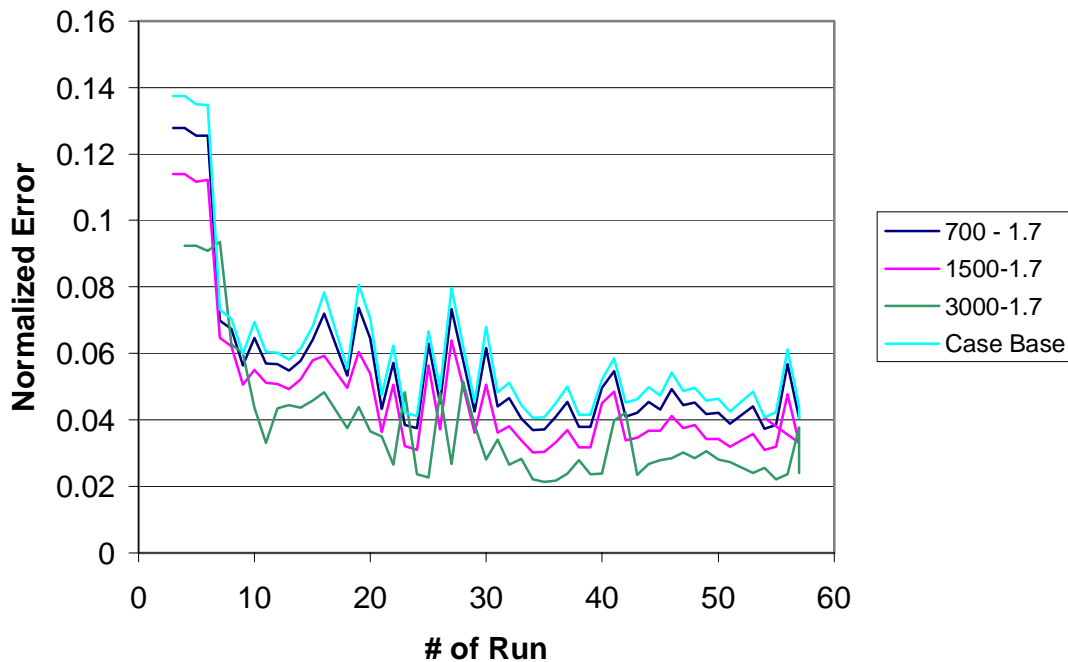
Fig. 3.10—Setting 3000 days as the end of "early time" minimizes error.

Fig. 3.10 shows the sensitivity to the definition of "early time" for a fixed early-data weighting factor of 1.7. A value of 3000 days as the end of early data and an ealy-data weighting factor of 1.7 produced the lowest error of the alternatives considered.

We found that we had to treat water cut carefully to avoid meaningless results. Reported values of WCT were as small as approximately 10^{-6}. When we normalized the errors, dividing the difference between observed and simulated values by such small observed values would have generated enormous errors. Further, such small observed values make no sense considering the accuracy and precision of field methods to measure water cut. Therefore, to avoid generating misleading errors we included WCT data only when the observed water cut was larger than 5%.

In calculating the error in GOR, we found that we needed to include neither restrictions, as with WCT, nor time-varying weighting factors, as with BHP.

In the error calculation procedure, we generated spreadsheet tables that contained all the simulated data for each run. Approximately 150,000 simulated data points for all variables, dates and runs were generated. These results had to be correlated with the much more modest number of observed data points available, about 1,500 values. Unfortunately, the simulation results were not reported at the same dates for all (i.e., the time step size sequence varied in different runs). This particularity has been the runs attributed to different convergence rates in the different runs. We developed a Visual Basic routine to compare dates and thus to resolve this difficulty.

Calculated errors are shown in **Table 3.2** and in **Figs. 3.11 to 3.14**.

TABLE 3.2 – CALCULATED ERRORS

RUN	ERROR BHP	ERROR WCT	ERROR GR	TOTAL ERROR
3	0.1273	1.6345	0.2133	0.2867
4	0.1273	1.6345	0.2146	0.2868
5	0.1249	1.6341	0.2189	0.2852
6	0.1251	1.6339	0.2202	0.2855
7	0.0695	1.3728	0.2645	0.2193
8	0.0669	1.3253	0.2417	0.2103
9	0.0559	1.1036	0.2576	0.1809
10	0.0632	1.2199	0.2927	0.2018
11	0.0564	1.1740	0.2424	0.1868
12	0.0562	1.1514	0.2308	0.1832
13	0.0543	1.1622	0.2289	0.1826
14	0.0574	1.0839	0.2220	0.1765
15	0.0637	1.0298	0.2262	0.1766
16	0.0702	1.1309	0.2214	0.1914
18	0.0529	1.1528	0.2603	0.1837
19	0.0720	1.0915	0.2167	0.1884
20	0.0633	1.0717	0.2184	0.1796
21	0.0427	1.0902	0.2244	0.1657
22	0.0573	1.1577	0.2203	0.1836
23	0.0378	1.1368	0.2437	0.1683
24	0.0368	1.1232	0.2426	0.1660
25	0.0622	1.3208	0.2522	0.2071
26	0.0440	1.0919	0.2329	0.1677
27	0.0728	1.4838	0.2362	0.2303
28	0.0570	1.3123	0.2463	0.2015

TABLE 3.2 Continued

RUN	ERROR BHP	ERROR WCT	ERROR GR	TOTAL ERROR
29	0.0415	1.1701	0.2459	0.1748
30	0.0605	1.1513	0.2125	0.1848
31	0.0431	1.1021	0.2336	0.1680
32	0.0455	1.1086	0.2330	0.1706
33	0.0398	1.1985	0.2456	0.1763
34	0.0361	1.2771	0.2412	0.1807
35	0.0364	1.1492	0.2423	0.1682
36	0.0400	1.1365	0.2397	0.1696
37	0.0444	1.1516	0.2466	0.1753
38	0.0373	1.1000	0.2366	0.1635
39	0.0374	1.1000	0.2365	0.1635
40	0.0490	1.1308	0.2434	0.1766
41	0.0542	1.1333	0.2359	0.1803
42	0.0403	1.1822	0.2433	0.1748
43	0.0412	1.1778	0.2464	0.1754
44	0.0443	1.1444	0.2459	0.1744
45	0.0428	1.1652	0.2438	0.1751
46	0.0486	1.2945	0.2479	0.1931
47	0.0439	1.2808	0.2446	0.1877
48	0.0449	1.2951	0.2448	0.1899
49	0.0409	1.2268	0.2408	0.1794
50	0.0411	1.2209	0.2440	0.1794
51	0.0380	1.2221	0.2388	0.1765
52	0.0949	1.2085	0.1903	0.2158
53	0.0430	1.1600	0.2103	0.1714
54	0.0366	1.1114	0.2308	0.1635
55	0.0378	1.1227	0.2298	0.1655
56	0.0555	1.1646	0.2433	0.1852
57	0.0393	1.1190	0.2264	0.1660
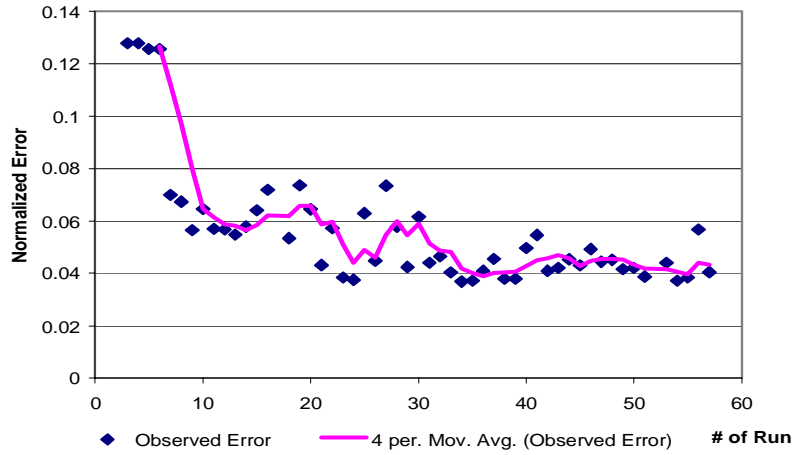
Fig. 3.11—Pressure errors decreasing with time.
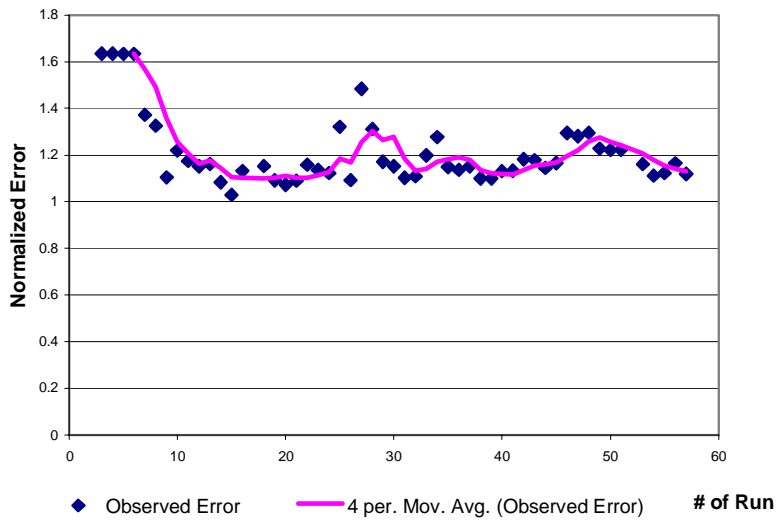
Fig.3.12—Water/cut doesn't show significant improvement.
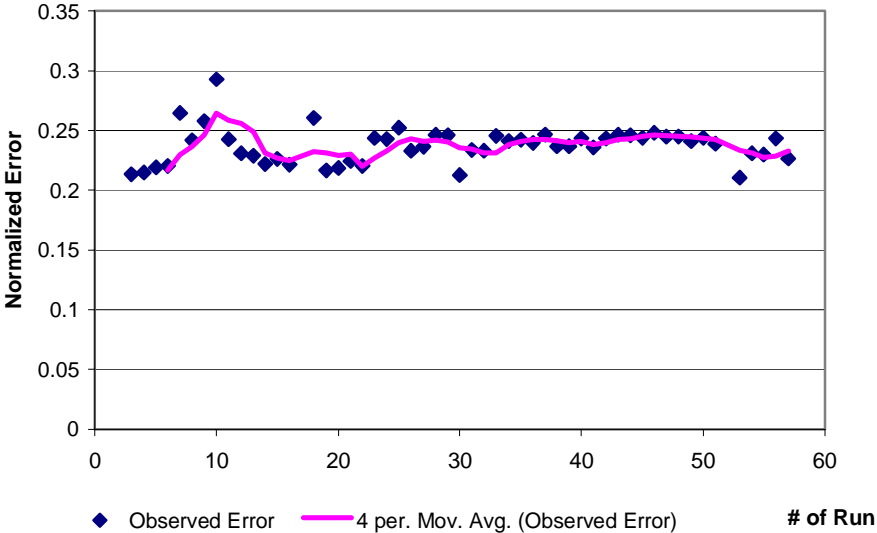
Fig. 3.13—GOR errors do not improve with time.
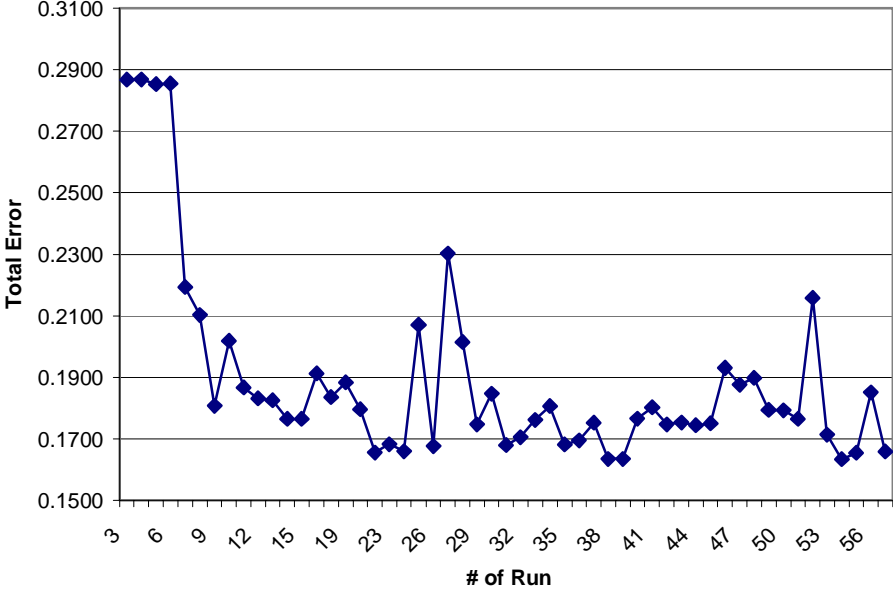
Fig. 3.14—Total error evolving with runs.

The observations used to compute errors in the mismatches are discussed in the following sub-sections.

Pressures. Static pressures from only 4 wells (3, 6, 7, and 12) were available. Wells 12 and 3 are located in Sector 1 of the reservoir which does not exhibit the same pressure trend as the rest of the reservoir. The error in the mismatch of these pressures match was computed using the average pressure of Sector 1 (dark sector shown in **Fig. 3.15).**
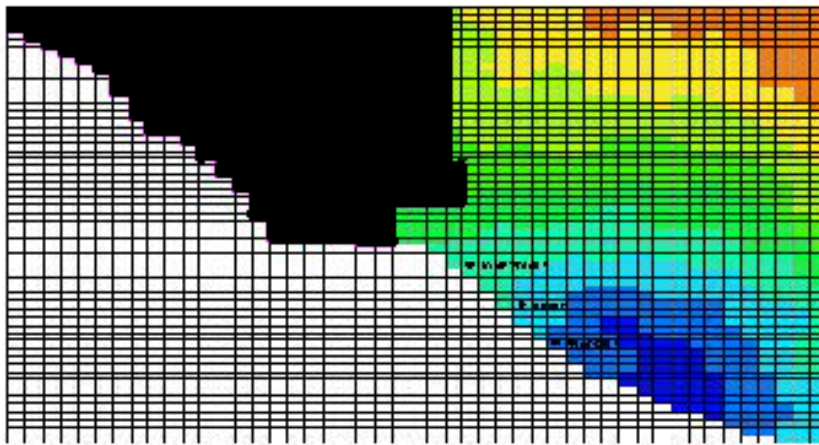
Fig. 3.15—Wells 12 and 3 located in Sector 1 (dark area in left side).

The error in the mismatch of wells 6 and 7 was computed by comparing their static pressures with the average pressure for the entire field.

Water Cuts. Produced water cut data were available for wells 2, 3, 6, 7, 9, 12 and 25. We analyzed each well individually.

Gas-Oil Ratio. We computed the error in GOR from the total field measurements. We had no information about where the gas measurements were made.

During the history matching process, a predictive run for the time period 1 September 2001 (end of history) to 1 September 2009 was made. For each of these forecasts, the cumulative oil production, called "Marginal Cumulative Oil Production," was recorded. These forecasts are summarized in the second column of the **Table 3.3.** The column "Cumulative Oil Production" represents the cumulative oil produced from 1987 to 2009.

TABLE 3.3 – CUMULATIVE OIL PRODUCTION

RUN	Marginal Cumulative Oil Production (STB)	Cumulative Oil Production (STB)
3	362,170	7,207,510
4	3,122,490	11,670,900
5	3,483,750	11,670,900
6	1,634,590	9,821,740
7	1,569,450	9,756,600
8	1,336,840	9,235,390
9	723,520	7,483,890
10	405,000	3,750,970
11	1,389,160	8,929,880
12	1,337,950	8,862,620
13	1,390,940	8,843,870
14	1,369,930	8,771,900
15	1,443,180	9,252,300
16	611,880	7,231,700
18	876,060	8,024,700
19	1,259,330	8,199,840
20	1,272,490	8,195,340
21	1,317,680	8,165,930
22	1,470,530	8,748,460
23	1,851,680	9,534,620
24	1,821,930	9,564,710
25	1,868,170	9,986,710
26	1,762,360	9,612,960
27	2,765,150	9,912,180
28	2,323,190	10,018,800
29	1,786,200	9,464,470
30	1,915,190	9,502,530
31	1,767,470	9,611,070

TABLE 3.3 Continued

RUN	Marginal Cumulative Oil Production (STB)	Cumulative Oil Production (STB)
32	1,766,150	9,618,150
33	1,762,990	9,625,300
34	1,751,770	9,672,500
35	1,712,380	9,634,990
36	1,969,890	9,955,690
37	2,068,110	9,965,590
38	1,988,660	9,870,750
39	1,989,780	9,871,870
40	2,164,530	9,839,970
41	2,075,360	9,895,980
42	1,987,220	9,946,390
43	2,019,860	9,697,930
44	2,070,960	9,968,770
45	2,025,040	10,024,000
46	2,216,740	10,223,600
47	2,173,440	10,220,500
48	2,168,590	10,206,700
49	2,228,920	9,975,780
50	2,203,700	10,115,700
51	2,146,640	10,022,700
52	2,692,090	9,762,750
53	2,405,430	9,855,720
54	1,971,550	9,929,790
55	1,944,270	9,978,860
56	2,150,970	10,310,500
57	1,801,090	9,876,510
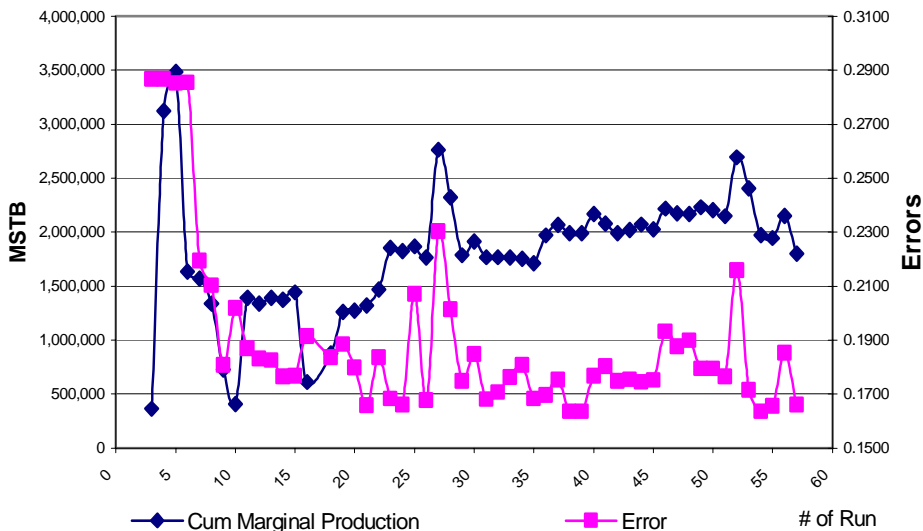
Fig. 3.16—Marginal cumulative oil production correlates well with total error.

The values of Marginal Cumulative Oil Production proved to be very sensitive to the errors computed from the history match (**Fig. 3.16**).

As we noted in Chapter II, if we assume a Gaussian distribution of the likelihood of mismatch errors, the probability function is exponential. In our case we compute the likelihood of each run as:

$$f\left(parameters\right) = c\exp[-error)] \dots\dots\dots\dots\dots\dots\dots\dots\dots\dots\dots\dots\dots\dots\dots\dots\dots\dots\dots(10)$$

c is a normalization factor and depends on the range of errors considered. With this approach, we found calculated the likelihood of weighting factors for all runs and summarized them in **Table 3.4.**

TABLE 3.4 – LIKELIHOOD DETERMINATION

RUN	ERROR TOTAL	WEIGHTING FACTOR
3	0.2867	0.5937
4	0.2868	0.5930
5	0.2852	0.6016
6	0.2855	0.6003
7	0.2193	1.0381
8	0.2103	1.1066
9	0.1809	1.3363
10	0.2018	1.1715
11	0.1868	1.2893
12	0.1832	1.3179
13	0.1826	1.3227
14	0.1765	1.3705
15	0.1766	1.3702
16	0.1914	1.2532
18	0.1837	1.3140
19	0.1884	1.2767
20	0.1796	1.3458
21	0.1657	1.4568
22	0.1836	1.3144
23	0.1683	1.4358
24	0.1660	1.4538
25	0.2071	1.1311
26	0.1677	1.4405
27	0.2303	0.9577
28	0.2015	1.1742
29	0.1748	1.3844
30	0.1848	1.3053
31	0.1680	1.4381
32	0.1706	1.4178
33	0.1763	1.3725
34	0.1807	1.3374
35	0.1682	1.4364
36	0.1696	1.4255
37	0.1753	1.3803
38	0.1635	1.4736
39	0.1635	1.4735
40	0.1766	1.3697
41	0.1803	1.3409
42	0.1748	1.3843
43	0.1754	1.3797
44	0.1744	1.3871
45	0.1751	1.3817
46	0.1931	1.2393
47	0.1877	1.2822
48	0.1899	1.2648

TABLE 3.4 Continued

RUN	ERROR TOTAL	WEIGHTING FACTOR
49	0.1794	1.3474
50	0.1794	1.3477
51	0.1765	1.3708
52	0.2158	1.0645
53	0.1714	1.4109
54	0.1635	1.4740
55	0.1655	1.4583
56	0.1852	1.3022
57	0.1660	1.4543

The average error and standard deviation for each run included information from the run and from all previous runs. For example the average value indicated in **Table 3.5** for run 6 is the average for runs 3, 4, 5 and 6 and the standard deviations for these same runs. (We did not include runs 1 and 2 in our analysis.) The weighting factors or normalized likelihoods are normalized to sum to unity in calculation of both averages and standard deviations.

We will consider an example. We completed our analysis of run 4 with forecasted oil production of 362,170 STB and a likelihood of 0.5937, and run 5, with a forecasted oil production of 3,122,490 STB and a likelihood of 0.5930. Normalizing 0.5937 and 0.5930 to add to unity results in the weighting factors of 0.50029 and 0.49970 respectively for these two runs and the weighted average oil forecast is then 1,741,416 STB.

The general formula for the weighted average can be expressed as follows:

$$X_{weighted} = \frac{1}{n} \sum_{i=1}^{n} w_i X_i \dots\dots\dots\dots\dots\dots\dots\dots\dots\dots\dots\dots\dots\dots\dots\dots\dots\dots\dots\dots\dots\dots.(11)$$

We calculated the standard deviations in forecasted oil production in a similar way. The theoretical basis for this methodology can be found in Sachs.[15]

The sample variance is generally calculated as follows:

$$S = \sqrt{\left(\frac{1}{n-1}\right)\sum_{i=1}^{n}(X_i - \overline{X})^2} \quad \dots\dots\dots\dots\dots\dots\dots\dots\dots\dots\dots\dots\dots \quad (12)$$

We can use the same weighting factor as before for each of the terms in the sum. The result is:

$$S_{weighted} = \sqrt{\left(\frac{1}{n-1}\right)\sum_{i=1}^{n} w_i (X_i - \overline{X})^2} \quad \dots\dots\dots\dots\dots\dots\dots\dots\dots\dots\dots \quad (13)$$

Eq. 13 allows us to calculate the weighted standard deviations, tabulated in **Table 3.5**.

Finally, we assumed the cumulative probability distributions are normal, and from them we calculated P90 ranges using weighted mean and standard deviations. We present and discuss the results later in this chapter.

In our analysis of the Green Canyon Field, we found a strong correlation between cumulative oil production forecasted for the period 2001-2009 ("Marginal Cumulative Production") and error. In this chapter, we will explain how we used this observation as our basis to quantify the uncertainty in our production forecasts.

Once errors became available, we assumed a Gaussian distribution for the errors, and we computed a likelihood of each run using **Eq. 10.**

We normalized the likelihood to compute the cumulative mean and standard deviation of the oil production forecasts. The "cumulative mean" and "cumulative standard deviation" include weighted values of means and standard deviations from all the runs available at the point that we make the calculation. For example, when we analyze run 35, we consider all runs from the start (run 3) to run 35. Results obtained in this way are summarized in **Table 3.5.**

TABLE 3.5 – AVERAGES AND STANDARD DEVIATIONS

RUN	Marginal Cum Production STB	Cum. Average Average STB	Weighted Average STB	Weighted Standard Deviation	Non-Weighted Standard Deviation
3	362170	362170	362,170	0	0
4	3122490	1742330	1,741,486	1,951,841	1,951,841
5	3483750	2322803	2,327,632	1,706,609	1,707,539
6	1634590	2150750	2,153,465	1,434,841	1,436,037
7	1569450	2034490	1,976,538	1,199,833	1,270,525
8	1336840	1918215	1,820,390	1,069,445	1,171,540
9	723520	1747544	1,570,678	1,064,648	1,160,885
10	405000	1579726	1,376,732	1,076,235	1,174,919
11	1389160	1558552	1,378,655	980,290	1,100,871
12	1337950	1536492	1,373,095	904,598	1,040,253
13	1390940	1523260	1,375,247	843,062	987,846
14	1369930	1510483	1,374,656	790,878	942,913
15	1443180	1505305	1,381,504	747,093	902,964
16	611880	1441489	1,317,053	747,581	899,800
18	876060	1403794	1,281,456	726,216	879,274
19	1259330	1394765	1,279,847	697,268	850,226
20	1272490	1387572	1,279,323	670,241	823,762
21	1317680	1383689	1,282,068	644,323	799,337
23	1851680	1408321	1,319,595	637,031	784,200
24	1821930	1429001	1,351,010	627,362	768,867
25	1868170	1449914	1,375,004	621,780	755,502
26	1762360	1464116	1,396,616	609,685	740,297
27	2765150	1520683	1,445,562	653,079	772,479
28	2323190	1554120	1,482,431	663,242	773,055
29	1786200	1563404	1,496,766	649,807	758,200
30	1915190	1576934	1,514,591	640,829	746,078
31	1767470	1583991	1,525,927	627,823	732,508
32	1766150	1590496	1,536,095	615,716	719,639
33	1762990	1596444	1,545,026	604,591	707,397
34	1751770	1601622	1,552,662	594,162	695,672
35	1712380	1605195	1,558,757	583,090	684,268
36	1969890	1616592	1,573,758	577,175	676,222
37	2068110	1630274	1,590,627	574,064	670,197
38	1988660	1640815	1,604,618	568,328	662,820
39	1989780	1650785	1,617,696	562,666	655,658
40	2164530	1665056	1,634,428	561,828	651,872
41	2075360	1676145	1,647,251	558,390	646,284
42	1987220	1684331	1,657,161	552,969	639,485
43	2019860	1692935	1,667,401	548,245	633,298
44	2070960	1702385	1,678,538	544,519	627,977
45	2025040	1710255	1,687,810	539,945	622,122
46	2216740	1722314	1,700,206	539,532	619,438
47	2173440	1732805	1,711,410	537,887	615,874
48	2168590	1742710	1,721,843	536,026	612,205

TABLE 3.5 Continued

RUN	Marginal Cum Production STB	Cum. Average Average STB	Weighted Average STB	Weighted Standard Deviation	Non-Weighted Standard Deviation
49	2228920	1753514	1,733,877	535,175	609,533
50	2203700	1763301	1,744,772	533,582	606,366
51	2146640	1771457	1,754,032	530,754	602,340
52	2692090	1790637	1,770,522	540,603	610,534
53	2405430	1803184	1,784,979	542,738	610,492
54	1971550	1806551	1,789,314	537,010	604,699
55	1944270	1809251	1,792,795	531,324	598,932
56	2150970	1815823	1,799,841	528,354	594,921
57	1801090	1815545	1,799,868	522,544	589,177

The weighted standard deviations are smaller than the non-weighted standard deviations. In both cases, standard deviations trend lower as information from more runs becomes available (**Fig. 3.17**).

Fig. 3.18 shows the trend in forecasted production (2001-2009). As can be seen both weighted and non-weighted average converge to the same values when numerous runs with similar errors and predicted production values become available. The final value of convergence eventually would be the one forecasted with the best match approach.
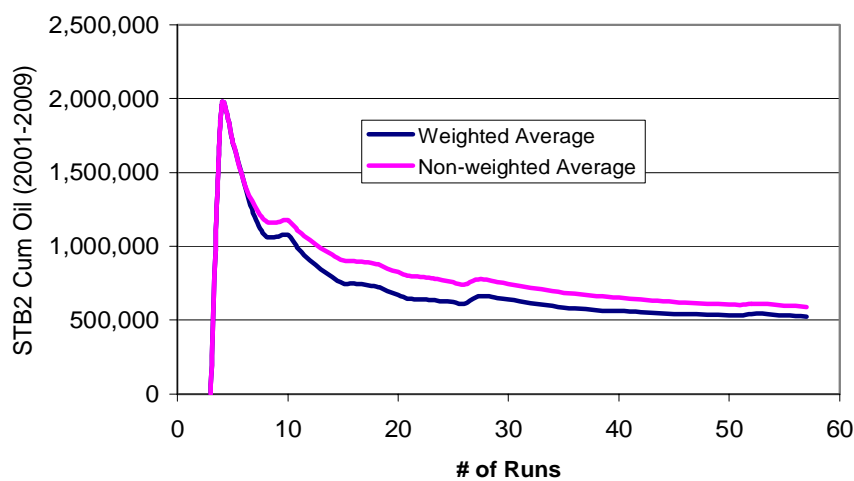

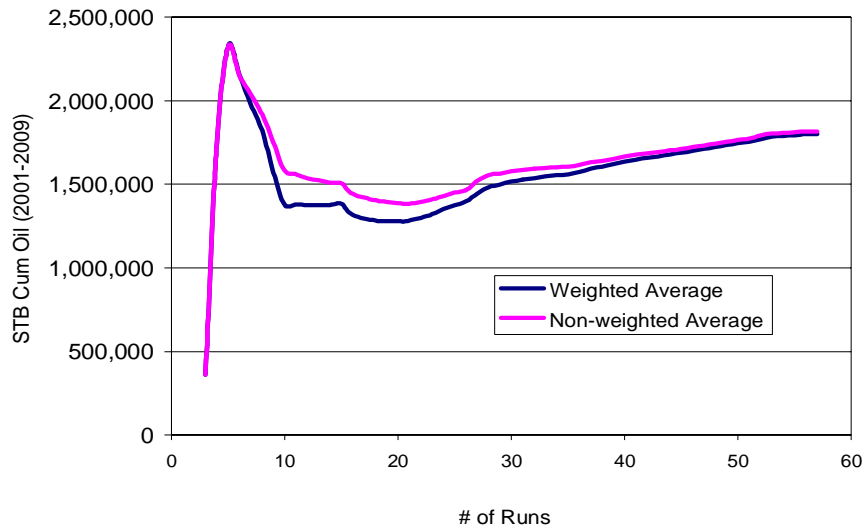**Fig. 3.17 – Weighted standard deviation is smaller than non weighted.**

Fig. 3.18 - Shows sets of weighted and non weighted mean values.

Using the weighted average mean and standard deviation, again assuming a normal distribution of Marginal Cumulative Oil or, more simply, reserves, we can compute the P-90 range after each history match run. These P-90 range values are shown in **Table 3.6** and **Fig 3.19.**

TABLE 3.6 – RANGES OF P-90 FOR THE CUMULATIVE OIL PREDICTED FOR 2001-2009

RUN	Maximum STB	Minimum STB	Average STB
4	4,951,977	0	1,741,486
5	5,134,754	0	2,327,632
6	4,513,568	0	2,153,465
7	3,950,087	2,990	1,976,538
8	3,579,470	61,310	1,820,390
9	3,321,867	0	1,570,678
10	3,146,980	0	1,376,732
11	2,991,087	0	1,378,655
12	2,861,025	0	1,373,095
13	2,761,960	0	1,375,247

TABLE 3.6 Continued

RUN	Maximum STB	Minimum STB	Average STB
14	2,675,535	73,777	1,374,656
15	2,610,362	152,646	1,381,504
16	2,546,714	87,391	1,317,053
18	2,475,974	86,937	1,281,456
19	2,426,749	132,944	1,279,847
20	2,381,770	176,875	1,279,323
21	2,341,884	222,251	1,282,068
22	2,320,899	266,097	1,293,498
23	2,345,375	310,986	1,328,180
24	2,360,615	354,196	1,357,406
25	2,375,213	384,570	1,379,891
26	2,377,491	422,902	1,400,196
27	2,494,273	399,188	1,446,730
28	2,546,916	416,876	1,481,896
29	2,540,336	450,946	1,495,641
30	2,544,145	481,412	1,512,778
31	2,535,249	512,245	1,523,747
32	2,526,571	540,667	1,533,619
33	2,518,172	566,467	1,542,320
34	2,509,554	590,016	1,549,785
35	2,498,384	613,176	1,555,780
36	2,504,187	636,608	1,570,398
37	2,516,318	657,376	1,586,847
38	2,521,416	679,667	1,600,542
39	2,525,718	701,021	1,613,370
40	2,541,374	718,132	1,629,753
41	2,548,954	735,752	1,642,353
42	2,550,449	753,820	1,652,135
43	2,553,382	771,106	1,662,244
44	2,558,808	787,666	1,673,237
45	2,560,997	803,837	1,682,417
46	2,572,979	816,292	1,694,636
47	2,581,790	829,615	1,705,702
48	2,589,475	842,566	1,716,021
49	2,600,408	855,429	1,727,918
50	2,608,996	868,418	1,738,707
51	2,613,952	881,855	1,747,903
52	2,646,611	881,687	1,764,149
53	2,664,809	892,086	1,778,447
54	2,660,147	905,539	1,782,843
55	2,654,682	918,115	1,786,398
56	2,657,147	929,712	1,793,430
57	2,647,997	939,186	1,793,591

The range of reserve estimates is almost constant after run 40. We associate this behavior with the observed difficulty of achieving better matches. We attribute that difficulty, in turn, to the selection of a particular static model that was the basis for all history matching in this project.
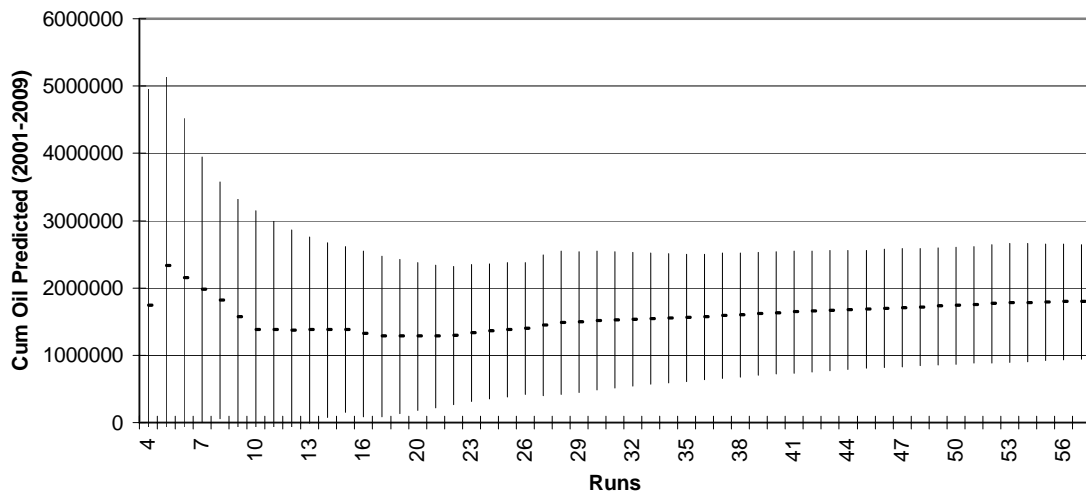

Fig 3.19 – P 90 ranges of estimated reserves.

CHAPTER IV

SUMMARY AND CONCLUSIONS

Our study of the Green Canyon field led us to several conclusions that we tentatively consider to be general. First, the methodology we discussed in Chapter III should prove generally useful to quantify uncertainty in reserve forecasts when only limited data are available and limited computational time is allowed for a study. We drew this conclusion because the weighted standard deviation was reduced when we assigned likelihoods to each history match run based on its closeness to the observed dynamic data.

We also conclude that the estimation of likelihood of each model based only on posteriori probabilities (observed data) can lead to a poor estimate of uncertainty for a given model. Geological knowledge should be included in the likelihood estimates to quantify uncertainty more realistically.

The determination of uncertainty in our predictions needs to be based on the generation of as many realizations as feasible and on making predictions with each realization. All realizations are possible from a statistical point of view and must be given certain likelihoods. These likelihoods can be assigned when we observe how closely the realizations model actual reservoir behavior.

Weighting results as new history matching information becomes available allows an early evaluation of the uncertainty in forecasts based on history matching performance. Further, a complete characterization of uncertainty requires the use of different geological realizations with their respective *a priori* probabilities.

Parameters used to define the objective function are chosen from available observed data and should efficiently describe pressures and rates combined in such a way that they describe the movement of all fluid phases present throughout the reservoir, up the wells and through the separators.

The objective function used to compute the mismatch during history matching should be representative of the variables considered by engineers who perform the history

matching, as was the case for the Green Canyon Field. Still, we must recognize that the visual improvement in matches from run to run is sometimes rather subjective and we may not be able to describe it completely by any objective function.

We also reached certain conclusions specific to the Green Canyon Field. Most notably, the error in gas/oil ratios and water cuts could not be reduced substantially during history matching. We believe that this outcome can be corrected only by modifying the geological model.

The history matches showed little improvement after run 40. We suspect that, when engineers reach a point of "acceptable" results, they become reluctant to make substantial modifications to their models.

The pressure error decreased markedly as additional runs were made, as **Fig. 3.11** shows. WCT and GOR oscillated without any substantial improvement with succeeding runs as **Fig. 3.13** and **Fig. 3.14** demonstrate. We attribute this behavior to the selection of an incorrect geologic model. The movement of water and gas within the reservoir depend on the reservoir geometry and thus cannot be reproduced adequately with an incorrect geological model. Pressure behavior within the reservoir is related to the amount of fluid in the pore space network and can be modified by varying parameters, such as net-to-gross ratio and perforation intervals, to obtain better matches.

Standard deviation decreased monotonically during history matching for both weighted and non-weighted errors. The weighted-standard deviation is smaller than the non-weighted, whereas the averages converge to a common value after several runs as shown in **Fig. 3.18.**

REFERENCES

1. Berteig, V., Halvorsen, K.B., More, H., Hoff, A.K., Jorde, K. *et al.*: "Prediction of Hydrocarbon Pore Volume With Uncertainties," paper SPE 18325, presented at the 1988 SPE Annual Technical Conference and Exhibition, Houston, 2-5 October.

2. Floris, F.J. *et al.*: "Methods for Quantifying the Uncertainty of Production Forecasts: A comparative Study," *Petroleum Geosciences* (2001) **7**, 87-97.

3. Abrahamsen, P., Egeland, T., Lia, O., More, H.: "An Integrated Approach to Prediction of Hydrocarbon in Place and Recoverable Reserves With Uncertain Measures," paper SPE 24276 presented at the 1992 European Petroleum Computing Conference, Stavanger, 25-27 May.

4. Samson, P. Dubrule, O. and Euler, N.: "Quantifying the Impact of Structural Uncertainties in Gross-rock Volume Estimates," paper SPE 35535, presented at the 1996 European 3D Research Modeling Conference, Stavanger, 16-17 April.

5. Floris, F.J.T. and Peersmann, M.R..: "Uncertainty Estimation in Volumetrics for Supporting Hydrocarbon E&P Decision Making," *Petroleum Geosciences* (1998) **4**, 33.

6. Egberts, P.J.P., Brouwer, G.K. and Bos, C.F.M.: "History Matching and Forecasting With Uncertainty Quantification: A Real Case Study," paper presented at the 2002 EAGE European Association of Geoscientists and Engineers, Florence, Italy, 27th May.

7. Roggero, F. and Guerillot, D.: "Gradient Method and Bayesian Formalism Application to the Petrophysical Parameter Characterization," paper presented at the 1996 European Conference on the Mathematics of Oil Recovery, Leoben, Austria, 3-6 September.

8. Nepveu, M.: "Hydrocarbon Production Forecasting with Limited Data – How to Fill the Gaps," *Proc*., 7th European Conference on the Mathematics of Oil Recovery, Baveno, Italy (2000) V-5, 63.

9. Ramarao, B.S. *et al.*: "Pilot Point Methodology for Automated Calibration of an Ensemble of Conditionally Simulated Transmissivity Fields, Theory and Computational Experiments," *Water Resources Research* 1990, 31, 475.

10. Manceau, A.M., Mezghani, M., Zabalza, I., Roggero.F.: "Combination of Experimental Design and Joint Modeling Methods for Quantifying the Risk Associated With Deterministic and Stochastic Uncertainties –An Integrated Test Study," paper SPE 71620 presented at the 2001 SPE Annual Technical Conference and Exhibition, New Orleans, 30 September-3 October.

11. Roggero, F.: "Direct Selection of Stochastic Model Realizations Constrained to Historical Data," paper SPE 38731 presented at the SPE 1997 Annual Technical Conference and Exhibition, San Antonio, Texas, 5-8 October.

12. "Bayesian Well Log Inversion," Netherlands Institute of Geosciences Applied - TNO-NITG, www.nitg.tno.nl/eng/pubrels/infor_mation/ inf_archives/inf_nr8/nr8art1.shtml, December 2001.

13. Scales, J.A. and Snieder, R.: "To Bayes or not to Bayes," *Dept. of Geophysics and Center for Wave Phenomena, Colorado School of Mines* (1997), 1045.

14. Aniekwena, A.: "Green Canyon 18, Dynamic Simulation of the 8-Reservoir," MS thesis, Texas A&M U.,College Station, Texas (2003).

15. Sachs, L.: *Applied Statistics*, Springer Series in Statistics, Springer-Verlag, Berlin, Germany (1984) **1**, 77.

VITA

Name: Martin G. Alvarado

DOB: 04/25/1966

Place of Birth: Santa Fe, Argentina

Permanent Address: Pje J.R. Rodriguez 3534 (3000) – Santa Fe - Argentina

Education

Master of Science. Texas A&M. – Petroleum Engineering

BS. Industrial (Chemical) Engineering. Universidad Nacional de Rosario. Argentina

Experience

2002 - Research Assistant – Texas A&M – Reservoir Uncertainty Group

2000-2001   Senior Business Analysts. TCS. Buenos Aires

1998-2000.   Sales Manager. Nova Petrene (Former Phillips 66 do Brasil). Sao Paulo –
Drilling Specialties Sales

1995-1998.   Industrial Sales Manager – YPF – Buenos Aires

1992-1995.   Production Planning Manager. Economic evaluations. San Lorenzo
Refinery. San Lorenzo, Argentina